AMERICAN SOCIETY FOR MICROBIOLOGY | Journal of Virology®

VIRUS-CELL INTERACTIONS

Mouse Adenovirus Type 1 E4orf6 Induces PKR Degradation

Berto Tejera-Hernández,[a] Danielle E. Goodman,[a]* Juan M. Nevarez,[a] Katherine R. Spindler[a]

[a]Department of Microbiology and Immunology, University of Michigan, Ann Arbor, Michigan, USA

ABSTRACT Protein kinase R (PKR) is a cellular kinase involved in the antiviral response. The inactivation or inhibition of this protein is a conserved activity in DNA and RNA virus infections. In contrast to human adenovirus type 5, mouse adenovirus type 1 (MAV-1) inhibits PKR activity through proteasome-dependent degradation. However, the molecular mechanism by which this process takes place is not fully understood. We investigated whether ubiquitination, MAV-1 early region 1B 55k (E1B 55k), and early region 4 orf6 (E4orf6) play a role in PKR degradation in MAV-1 infection, because the enzyme 3 (E3) ubiquitin ligase activity with these viral proteins is conserved among the *Adenoviridae* family. We provide evidence that E4orf6 is sufficient to induce mouse PKR degradation and that proteasome pathway inhibition blocks PKR degradation. Inhibition of neddylation of cullin, a component of E3 ubiquitin ligase complex, blocked efficient PKR degradation in MAV-1-infected cells. Finally, we demonstrated that MAV-1 degradation of PKR is specific for mouse PKR. These results indicate that counteracting PKR is mechanistically different in two species of adenoviruses.

IMPORTANCE Viruses have evolved to counteract the immune system to successfully replicate in the host. Downregulation of several antiviral proteins is important for productive viral infection. Protein kinase R (PKR) is an antiviral protein that belongs to the first line of defense of the host. Because PKR senses dsRNA and blocks the cellular translation process during viral infections, it is not surprising that many viruses counteract this antiviral activity. We previously reported PKR degradation during mouse adenovirus type 1 (MAV-1) infection; however, the molecular mechanism of this activity was not fully known. This work provides evidence about the MAV-1 protein that induces PKR degradation and expands knowledge about involvement of the proteasome pathway.

KEYWORDS cullin, PKR, mouse adenovirus, proteasome, ubiquitination

Mouse adenovirus type1 (MAV-1; also known as MAdV-1) belongs to the *Adenoviridae* family. It is a nonenveloped virus with an icosahedral capsid containing a double stranded DNA genome of ~31 kbp (1, 2). Following intraperitoneal inoculation, MAV-1 infects primarily endothelial cells and macrophages and causes encephalitis in mice (3–6). Because information about human adenovirus (HAdV) pathogenesis is limited due to the high specificity of HAdV for the host, MAV-1 has been used as a model to understand adenoviral pathogenesis and persistence in animals (7–10). While HAdV and MAV-1 have many infection processes in common (11, 12), some aspects are different. For example, HAdVs circumvent the host antiviral response, induction of protein kinase R (PKR), by encoding small virus-associated (VA) RNAs (13, 14). However, MAV-1 does not encode VA RNAs (15). Recently we showed that the cellular protein PKR is degraded during MAV-1 infection, and the data suggested that the proteasome pathway is involved in this activity (16).

HAdV infections cause degradation of a variety of cellular substrates. HAdV assembles an enzyme 3 (E3) ubiquitin ligase complex that induces the polyubiquitination and degradation of multiple cellular proteins, including apoptosis and cell cycle regulators such

Editor Lawrence Banks, International Centre for Genetic Engineering and Biotechnology

Address correspondence to Katherine R. Spindler, krspin@umich.edu.

*Present address: Danielle E. Goodman, Bio-Rad Laboratories, Ann Arbor, Michigan, USA.

The authors declare no conflict of interest.

Received 30 November 2021
Accepted 12 February 2022
Published 14 March 2022

as p53 (17), DNA damage response components including Mre11 (18) and Bloom helicase (19), chromatin regulators (e.g., Tip 60) (20), and other proteins (21–23). To be degraded, most of these cellular substrates require the presence of and the interaction between two early viral proteins, HAdV early region 1B 55k (E1B 55k) and early region 4 orf6 (E4orf6). In transfection of human cells with MAV-1 genes, only mouse p53 has been demonstrated as a target of the MAV-1 E3 ubiquitin ligase complex, and both MAV-1 E1B 55k and E4orf6 were required (24).

PKR is a cellular protein that is part of the innate immune response. PKR senses dsRNA and is activated by autophosphorylation during stress conditions or viral infections, leading to phosphorylation of eIF-2α. This impairs eIF-2α activity (25), which results in the inhibition of protein synthesis and the induction of apoptosis (reviewed in Ref. 26). Also, PKR is involved in signal transduction and transcriptional control of the NF-κB pathway. This results in transcriptional regulation through the activation of cellular transcription factors controlling the expression of genes such as IRF-1, STATs, MAPKs and p53 (26, 27).

Although MAV-1 does not encode a VA RNA, we demonstrated that PKR is degraded during MAV-1 infection (16). To our knowledge, MAV-1 is the first DNA virus demonstrated to regulate PKR activity through degradation. Here, we investigated whether ubiquitination and MAV-1 E1B 55k and E4orf6 play a role in PKR degradation. Transfections of human and mouse cells with plasmids expressing mouse PKR, MAV-1 E1B 55k and MAV-1 E4orf6 showed that E4orf6 alone is sufficient to induce mouse PKR degradation. Proteasome inhibition with MG132 rescued PKR levels in those transfections, in agreement with observations in MAV-1-infected mouse cells (16). Cullin 2 is a component of the MAV-1 E4orf6 ubiquitin ligase complex (24). We used a mutant construct of MAV-1 E4orf6 in which the cullin-E4orf6 interaction is disrupted by three amino acid changes. Transfection of human and mouse cells with this mutant E4orf6 construct resulted in no degradation of mouse PKR, suggesting that the cullin-E4orf6 interaction is important for mouse PKR degradation by MAV-1. Finally, we demonstrated that human PKR is not degraded in MAV-1- or HAdV2-infected cells, in contrast to mouse PKR, which is degraded in MAV-1-infected mouse cells.

RESULTS

MAV-1 PKR degradation is proteasome-dependent in mouse 3T6 cells and requires cullin neddylation. PKR is degraded in several mouse cell types (C57BL/6 mouse embryo fibroblasts, CMT93 cells, and mouse macrophages) infected by MAV-1 (16). We performed experiments to confirm PKR degradation and the role of the proteasome pathway during MAV-1 infection in an additional cell type, a 3T6 mouse fibroblast cell line. Cells were infected for 24 h and treated with increasing concentrations of the proteasome inhibitor MG132 from 18–24 h postinfection (hpi) (Fig. 1A). Cells not treated with MG132 showed a decrease in PKR levels in infected cells compared to mock, as expected (Fig. 1A, lanes 1 and 5), confirming that PKR was degraded in MAV-1-infected cells. However, increasing doses of MG132 stabilized PKR in infected cells, showing a similar PKR accumulation to that in mock-infected cells at the highest MG132 concentration (Fig. 1A, lanes 4 and 8). Also, MG132 treatment did not affect viral early region 1A (E1A) protein accumulation (Fig. 1C, lanes 3–5), indicating that MG132 did not affect MAV-1 early gene expression. MG132 treatment did not alter PKR accumulation in mock-infected cells. Together, the results indicate that PKR is degraded during infection.

Cullins are required for the E3 ubiquitin ligase complex assembly. These cellular proteins are activated by a post-translational modification called neddylation, and this is necessary for the assembly of the E3 ubiquitin ligase complex (28–30). To analyze the effect of cullin neddylation on PKR degradation, we infected 3T6 cells with MAV-1 for 24 h or mock-infected control cells, and we treated cells with increasing concentrations of a neddylation inhibitor, MLN4924 (31, 32) (Fig. 1B). The inhibition of cullin neddylation affects all cullin RING ligases; we confirmed the effect of MLN4924 on cullin 2 neddylation by the loss of the slower migrating band (Fig. 1B, lanes 2–4, 6–8). As expected, we observed reduced PKR levels in infected untreated cells compared to

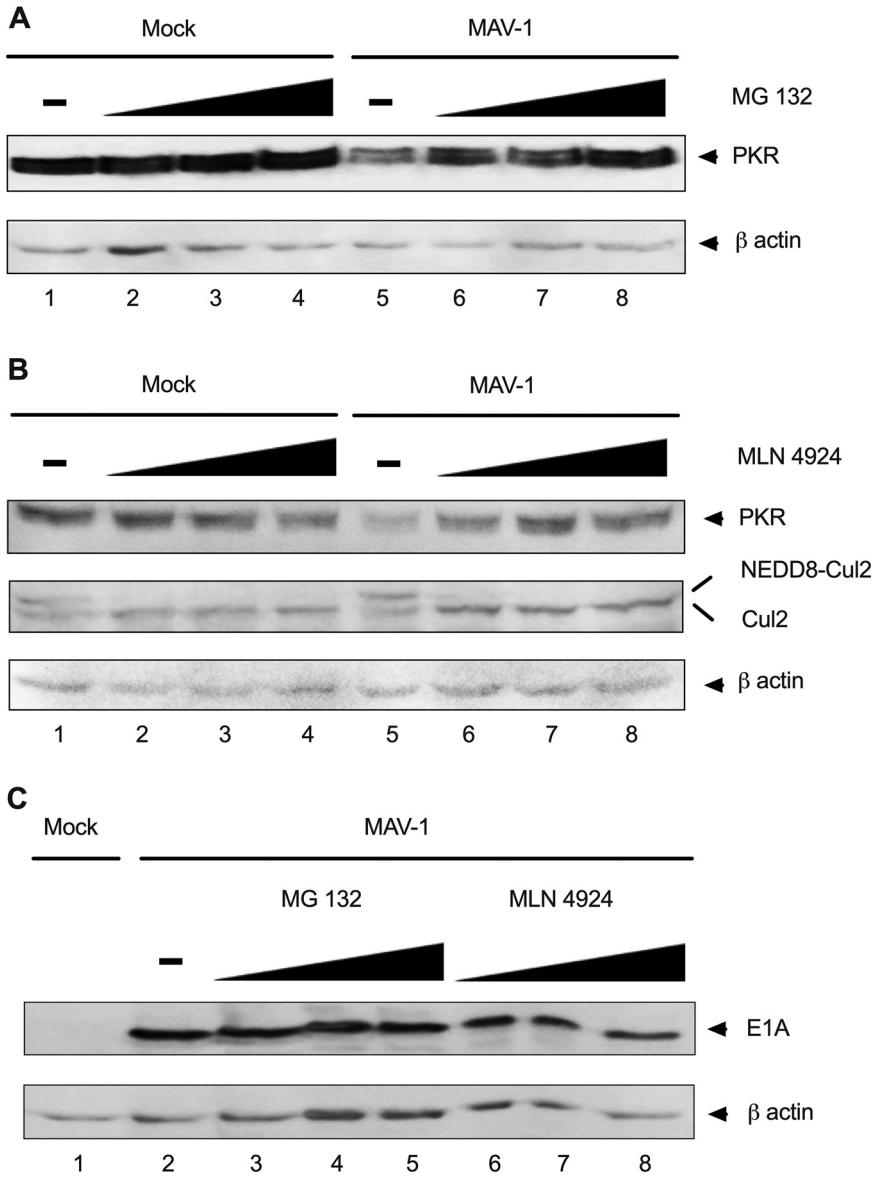

FIG 1 Effects on PKR degradation of inhibition of cullin-2 neddylation and proteasome activity in mouse-infected cells. Mouse 3T6 cells were infected with MAV-1, MOI 5 for 24 h. (A) Cells were treated with 0 (−), 1, 5 or 10 μM MG132 during the 6 h prior to harvesting. Total lysates were processed by immunoblot using anti-PKR and anti-β actin antibodies. (B) Cells were treated with 0 (−), 1, 3 or 5 μM MLN4924 for 24 h and harvested. Total lysates were processed by immunoblot using anti-PKR, anti-actin and anti-cullin 2 antibodies. (C) Total lysates from 0, 1, 5 or 10 μM MG132- and 0, 1, 3 or 5 μM MLN4924-treated cells were analyzed by immunoblot to detect the viral protein E1A. β-actin was used as the loading control. ImageJ analysis of E1A protein relative to β-actin indicated no changes in E1A accumulation (data not shown). Each panel is representative of at least three independent experiments.

mock infected (Fig. 1B, lanes 1 and 5). However, increasing MLN4924 concentrations stabilized PKR accumulation in infected cells (Fig. 1B, lanes 6–8). We saw no changes in early viral protein E1A expression (Fig. 1C, lanes 6–8), indicating that the neddylation inhibitor did not affect early viral gene expression. These data suggest that cullin neddylation is needed for PKR degradation in mouse-infected cells.

MAV-1 E4orf6 induces mouse PKR degradation in human and mouse transfected cells. HAdVs induce the degradation of multiple cellular substrates via two viral proteins, E1B 55k and E4orf6, facilitating viral replication. These viral proteins assemble an E3 ubiquitin ligase complex with cellular proteins including RunX1, elongins, and cullins, resulting in polyubiquitination of cellular substrates including p53 (33), Mre 11

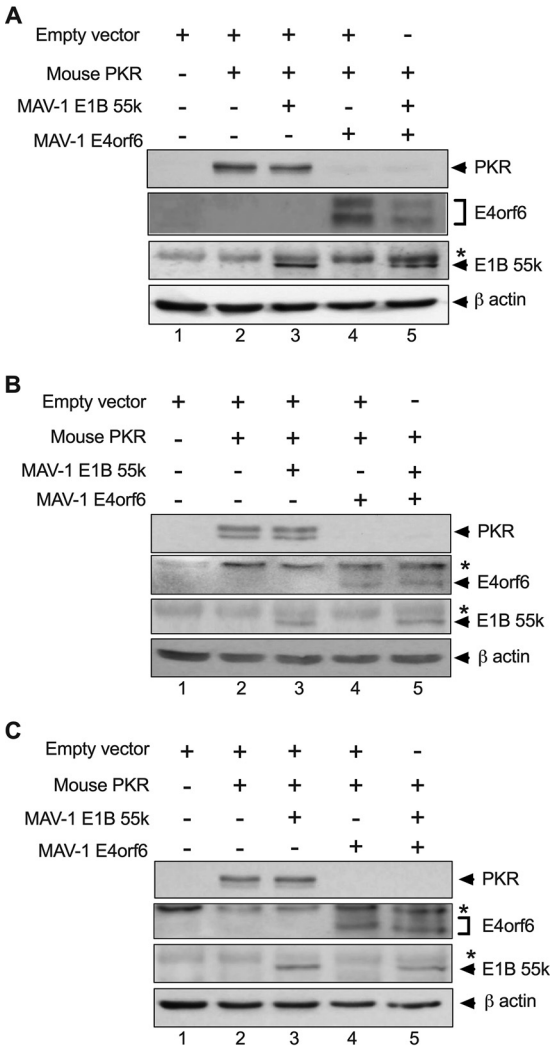

FIG 2 E4orf6 induces PKR degradation in transfected human and mouse cells. HT 1080 huPKR KO (A), PKR N$^-$ MEF (B), and PKR TKO MEF cells (C) were transfected with pFlag-PKR, pFlag-E1B 55k and pFlag-E4orf6 plasmids as indicated and harvested at 24 h posttransfection. Total lysates were analyzed by immunoblot using anti-PKR, anti-E4orf6 antiserum and anti-β actin antibodies. E1B 55k was detected by immunoprecipitation followed by immunoblot with anti-E1B 55k antiserum 80623. (+) indicates the plasmid is present, (−) indicates the plasmid is absent. *Nonspecific band. Each panel is representative of at least three independent experiments.

(18), and DNA ligase IV (34). The polyubiquitination leads to host protein degradation by the proteasome. For MAV-1, knowledge regarding this activity is limited. In human cells, MAV-1 induces mouse p53 degradation through the classical E3 ubiquitin ligase complex; MAV-1 E1B 55k and MAV-1 E4orf6 are required (24).

Initially, we suspected that both viral proteins (MAV-1 E1B 55k and MAV-1 E4orf6) were required to induce PKR degradation. We performed cotransfection experiments using a mouse cell line lacking full-length PKR. These cells, designated here as PKR N$^-$ embryo fibroblasts (MEFs), were derived from PKR knockout mice (35). In some conditions, these cells express an N-terminal deleted form of PKR (36). In our conditions, even this N-terminal deleted form of PKR was not detected (Fig. 2B, lane 1). We also used MEFs from a new line of mice in which mouse PKR was deleted by CRISPR/Cas9, designated herein as PKR TKO MEFs.

The mouse PKR gene was transfected alone or in combination with plasmids encoding MAV-1 E1B 55k and MAV-1 E4orf6 into either a human HT1080 PKR knockout cell line, PKR N$^-$ MEFs, or PKR TKO MEFs, to determine which viral proteins are required for

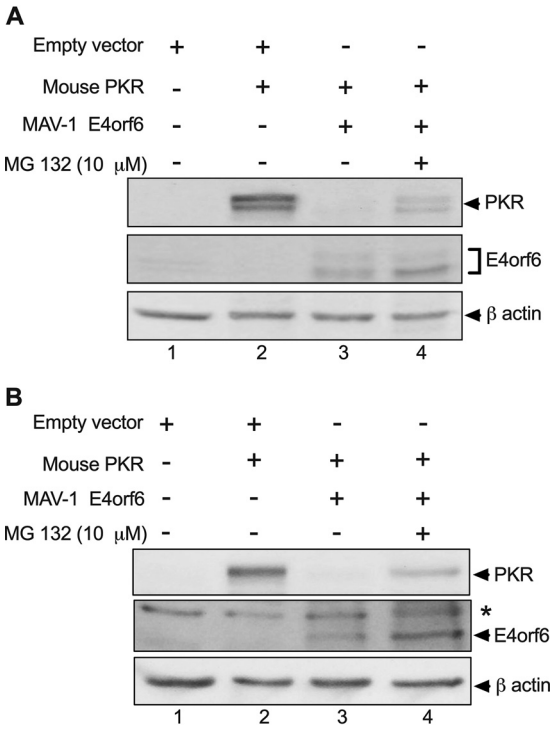

FIG 3 PKR is degraded through the proteasome pathway in transfected human and mouse cells. HT 1080 huPKR KO (A) and MEF N$^-$ (B) cells were transfected with pFlag-PKR and pFlag-E4orf6 plasmids at 24 h posttransfection. Cells were treated with 10 μM MG132, 6 h prior to harvesting, and samples were analyzed by immunoblot using anti-PKR and anti-E4orf6 antibodies. *Nonspecific band. Each panel is representative of at least three independent experiments.

PKR degradation (Fig. 2). We observed similar results in the three cell lines. In the presence of E1B 55k (Fig. 2A–C, lanes 3), PKR levels were very similar to transfection of PKR alone (Fig. 2A–C, lanes 2). However, PKR levels were significantly lower in the presence of E4orf6 (Fig. 2A–C, lanes 4 and 5). These data suggest that E4orf6 expression is sufficient to induce PKR degradation and that E1B 55k is not required or does not enhance PKR degradation. To confirm that E1B 55k was indeed produced in the transfected cells, immunoprecipitation assays were performed, and a specific band was detected in the expected lanes at the expected molecular weight (Fig. 2A–C, lanes 3 and 5). E4orf6 was detected directly by immunoblot (Fig. 2A, lanes 4–5). We detected a specific double band for E4orf6 in HT1080 PKR knockout cells, suggesting a possible post-translational modification in E4orf6-transfected human cells.

PKR is not degraded in human and mouse E4orf6-transfected cells when the proteasome pathway is blocked. The proteasome pathway is involved in PKR degradation in infected mouse cells (Fig. 1A and Ref. 16). We performed cotransfection experiments and MG132 treatment to confirm the proteasome pathway requirement for PKR degradation in the context of transfection with MAV-1 E4orf6 (Fig. 3). We confirmed in HT1080 PKR knockout and PKR N$^-$ cells that E4orf6 was sufficient to induce mouse PKR degradation (Fig. 3A and B, lanes 3). Cotransfecting E4orf6 and PKR in the presence of the proteasome inhibitor MG132 blocked degradation of PKR in both cell types (Fig. 3A and B, lanes 4). These data indicate that the proteasome pathway is involved in PKR degradation in transfected human and mouse cells.

Neddylation of cullin is required for PKR degradation. Cullins play an important role in E3 ubiquitin ligase complex assembly. As shown in Fig. 1B, cullin 2 neddylation was a requirement for PKR degradation in MAV-1-infected cells. Gilson et al. (24) showed that E4orf6-cullin 2 interaction-defective mutant orf6 proteins are impaired for binding to cullin 2. We cotransfected mouse PKR and either E4orf6 wild type (wt) or E4orf6-cullin 2 interaction-defective mutant plasmid constructs into HT1080 PKR

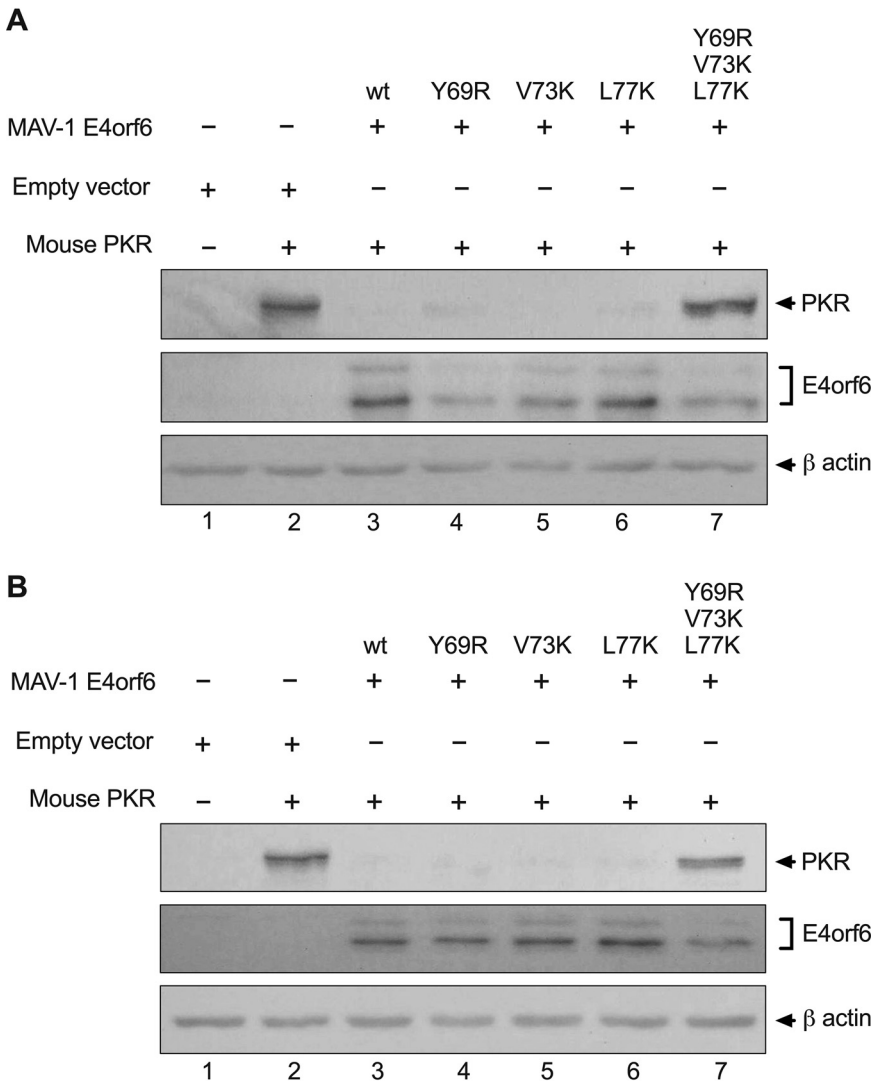

FIG 4 MAV-1 E4orf6-cullin 2 interaction is a requirement for PKR degradation in transfected human and mouse cells. HT 1080 huPKR KO (A) and PKR N^- MEF cells (B) were transfected with pFlag-PKR and MAV-1 E4orf6-encoding plasmids. wt: MAV-1 E4orf6 wild type; for each E4orf6 variant (lane 4–7), the amino acid position and the substitutions are listed. Lane 7 corresponds to the plasmid with all three amino acid changes, FLAGmE4orf6TMWT8. Cells were harvested 24 h posttransfection, and the samples were analyzed by immunoblot using anti-PKR and anti-E4orf6 antibodies. β actin was used as the loading control. *Nonspecific band. Each panel is representative of two independent experiments.

knockout and PKR N^- cells to determine whether the interaction of E4orf6-cullin 2 is a requirement for PKR degradation in transfected cells (Fig. 4). These mutants were originally designated as Y70R, V74K, and L78K based on the amino acids changed by the mutations (24). However, based on sequencing of cDNA clones (37) and inspection of splicing signals, the MAV-1 E4orf6 protein (corresponding to orf a/b in Ref. 37) has one fewer amino acid at the junction of the two open reading frames than other authors calculated (24). The numbering of the E4orf6 mutants is thus Y69R, V73K and L77K.

Transfection of mouse PKR into HT1080 PKR knockout and PKR N^- cells was successful, as shown in Fig. 4A, B, lanes 2. Mouse PKR was degraded in the presence of wt E4orf6 (Fig. 4 A, B, lanes 3) confirming the previous data (Fig. 2 and 3). PKR was also degraded in the presence of the E4orf6 proteins with single amino acid changes (Fig. 4A, B lanes 4–6). However, the efficiency of this activity was lower compared to wt E4orf6, because some PKR was detectable in lanes 4–6 (Fig. 4B). When all three amino acid changes were

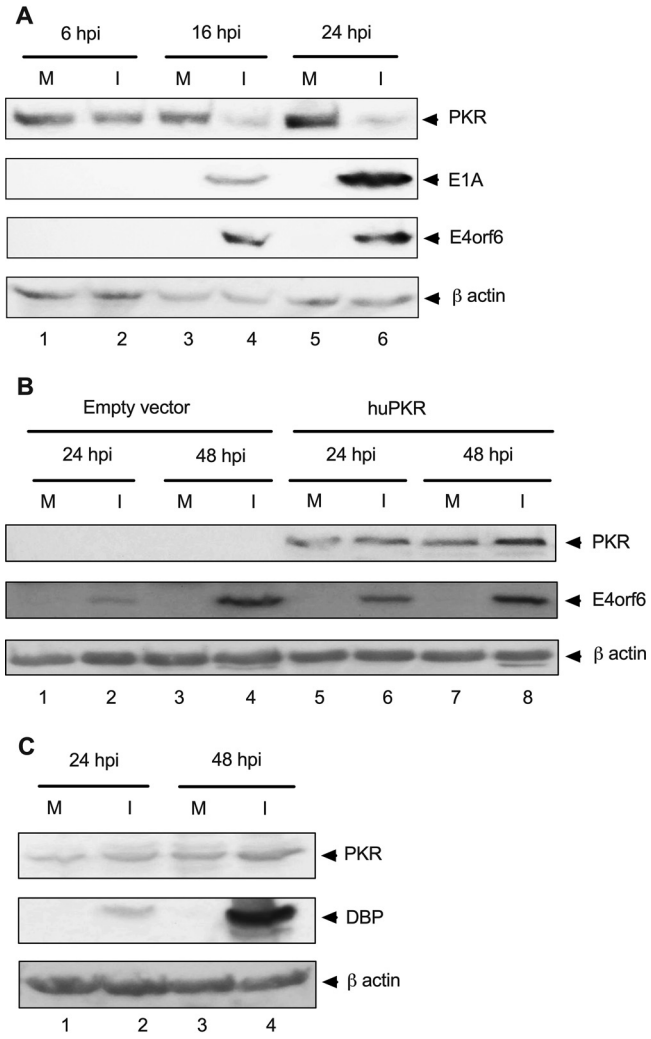

FIG 5 PKR degradation is a MAV-1-specific activity. (A) 3T6 mouse fibroblasts were infected with MAV-1 at MOI 5 and harvested 6, 16 and 24 hpi. (B) PKR C$^-$ MEF cells stably expressing empty vector (PKR$^{-/-}$ vector, lanes 1–4) or human PKR (PKR$^{-/-}$ huPKR, lanes 5–8) were infected with MAV-1, MOI 5 and harvested 24 and 48 hpi. (C) Human HT 1080 wild type cells were infected with HAdV 2, MOI 5 and harvested at 24 and 48 hpi. In all cases, total lysates were processed by immunoblot using anti-PKR, anti-MAV-1 E1A, anti-HAdV 2 DNA binding protein (DBP) and anti-β actin antibodies. M, Mock; I, Infected. Each panel is representative of at least three independent experiments.

present (lanes 7), PKR was not degraded; there was a similar level of PKR compared to the transfection of PKR alone (Fig. 4, lanes 2). These data indicate that the change of three amino acids in E4orf6 known to affect cullin 2 binding substantially affected the degradation of PKR in transfected human and mouse cells.

PKR degradation is a MAV-1-specific activity. PKR downregulation is an important activity during viral infections. To determine whether the PKR degradation by MAV-1 was specific to mouse PKR, we tested the ability of MAV-1 infection to induce huPKR degradation. First, we performed a time course experiment in mouse NIH 3T6 cells infected with MAV-1. PKR levels were lower at 16 and 24 hpi compared to mock infection (Fig. 5A, lanes 4 and 6), confirming the kinetics seen in other mouse cell types (16). We observed viral gene expression (E1A and E4orf6) at the same time points in which we detected PKR degradation (Fig. 5A, lanes 4 and 6). We then assayed whether MAV-1 induces human PKR (huPKR) degradation. MEF cells knocked out for mouse PKR expression stably transfected with the empty vector or huPKR (38) were infected with MAV-1 at 24 and 48 hpi (Fig. 5B). These cells, designated as C$^-$ PKR MEFs, can express a C-terminal truncated form of mouse PKR (36), but in our experimental conditions, this

protein was not detected (Fig. 5B, lanes 1–4). HuPKR was not degraded by MAV-1 infection (Fig. 5B, lanes 5–8). MAV-1 E4orf6 was detected at 24 and 48 hpi in empty vector cells (Fig. 5B, lanes 2 and 4) and huPKR-expressing cells (Fig. 5B, lanes 6 and 8), indicating that the lack of huPKR degradation was not due to a lack of E4orf6. To demonstrate that PKR degradation is a mechanism of regulation specific for MAV-1, we infected wild type HT1080 cells with HAdV2 at 24 and 48 hpi (Fig. 5C). HuPKR was not degraded in HAdV-2-infected cells. HT1080 cells were clearly infected, because the early viral protein DNA binding protein was detected.

DISCUSSION

PKR is an important component of the innate immune response. It counteracts viral infections by blocking protein translation and therefore viral replication. Inhibiting PKR antiviral activity is important for successful replication of DNA and RNA viruses (reviewed in Ref. 39). Our experiments confirm the finding that PKR is degraded through the proteasome pathway in MAV-1-infected cells; blocking this pathway resulted in little or no PKR degradation (Fig. 1 and 5A). The proteasome pathway is a well described mechanism by which the cell degrades cellular protein levels in different cell cycle stages, and viruses exploit this pathway to counteract the antiviral response (reviewed in Ref. 40). Also, in transfection experiments we showed that the early viral protein MAV-1 E4orf6 induced the degradation of PKR in human and mouse cells through the proteasome pathway (Fig. 2 and 3). The data showed that E1B 55k did not contribute to PKR degradation, indicating that MAV-1 assembles a different E3 ubiquitin ligase complex for PKR degradation than for mouse p53 degradation (24). For HAdV, both E1B 55k and E4orf6 are needed to polyubiquitinate and induce degradation of most cellular substrates (17–19, 34, 41). However, HAdV requires only E1B 55k to induce degradation of the antiviral protein Daxx, a component of PML nuclear bodies (42), whereas only E4orf6 is required for degradation of the cellular protein TOPBP1 (43). In transfected human cells, only MAV-1 E4orf6 is required to degrade mouse DNA ligase IV (24). There are no obvious protein sequence features among mouse DNA ligase IV, human TOPBP1 and mouse PKR that could explain their independence for E1B 55k degradation by adenoviruses.

The E3 ubiquitin ligase complex assembled by HAdV to induce the degradation of most cellular substrates requires the presence of E4orf6 and cullins. Most HAdVs use cullin 5, whereas MAV-1 uses cullin 2 (24). Gilson et al. (24) showed that three MAV-1 E4orf6 amino acid changes (Y69R, V73K, L77K) impair the interaction of E4orf6 with cullin 2. We determined the effect of the interaction of E4orf6 and cullin 2 on PKR degradation using wild type and variant E4orf6 proteins. Our data suggest that the E4orf6-cullin 2 interaction is required for efficient PKR degradation in human and mouse transfected cells (Fig. 4). The E4orf6 variant with all amino acid changes, Y69R/V73K/L77K, showed the most drastic phenotype: PKR was not degraded. Inhibition of neddylation by treatment with MLN4924 blocked PKR degradation in infected cells (Fig. 1). This suggests that cullin 2 neddylation contributes to PKR degradation. We cannot rule out the possibility that neddylation of other cullins or other proteins that could be involved in PKR degradation (32) was also affected in this experiment.

To our knowledge, MAV-1 is first described DNA virus in which PKR is regulated by degradation, though PKR degradation occurs in infections with some RNA viruses, such as Rift Valley Fever virus and Toscana virus (44, 45). MAV-1 infection does not induce huPKR degradation in mouse cells stably expressing huPKR (Fig. 5). Human PKR and mouse PKR both have eIF-2α phosphorylation activity (46, 47) but they share only 56% identity and 69% similarity. The difference in protein sequence could explain why MAV-1 infection does not induce degradation of huPKR. Also, HAdV does not induce huPKR degradation in HT1080 cells (Fig. 5C), confirming that the mechanism of PKR downregulation in HAdV takes place through a degradation-independent mechanism, consistent with its dependence on VA-RNA (13, 14).

The PKR-activating dsRNA has not been definitively detected in adenovirus

infections, and the mechanism of PKR activation in HAdV remains unknown. It has been proposed that dsRNA is generated by annealing of mRNA transcripts from both strands of adenovirus DNA (14, 48), but convincing evidence for intermolecular dsRNA formation in adenovirus infections is lacking. Accumulation of dsRNA in adenovirus-infected cells has recently been shown with E4-defective HAdV mutants (49). This appears to be due to a deficiency in viral mRNA splicing in the E4 mutant infections, accompanied by PKR relocation to the nucleus. Also, either the absence of E1B 55k or E4orf6, or the inhibition of the E3 ubiquitin ligase complex results in the accumulation of dsRNA. Price et al. (49) propose that an efficient splicing process could explain the undetectable levels of dsRNA in wild type HAdV infection. It is not known whether very low (as yet undetectable) levels of dsRNA present in wild type HAdV infection are sufficient to cause the induction of PKR. In Zika virus infection, PKR is activated by mitochondrial RNA (mtRNA) when mitophagy is compromised, resulting in an increase of PKR-dependent chemokine expression (50). It is not known whether mtRNA is a significant source of dsRNA in adenovirus infections. In addition, PKR activation could occur in a dsRNA-independent manner; oxidative stress, endoplasmic reticulum stress and metabolic stress induce PKR activation (38, 51, 52).

Our data provide direct evidence of viral E4orf6 protein involvement in PKR downregulation in MAV-1 infection. However, there are questions remaining, including the effect of PKR degradation on expression of genes downstream of PKR. We have been unable to detect changes in eIF-2α phosphorylation in MAV-1 infections compared to mock-infected cells (data not shown). We hypothesize that a PKR degradation-defective mutant virus (e.g., E4orf6-deleted) could increase eIF-2α phosphorylation and possibly an increase of PKR-dependent chemokine expression, blocking virus replication. Such a mutant virus, coupled with true PKR knockout mice from which we generated the PKR-TKO MEFs used herein, will be useful in determining the importance of PKR degradation in natural infections.

MATERIALS AND METHODS

Cells, virus, and infections. NIH 3T6 fibroblasts (53) were grown in Dulbecco's modified Eagle medium (DMEM) plus 10% heat-inactivated calf serum. PKR N- MEF cells were obtained from Robert Silverman, Cleveland Clinic Foundation (54). These cells were originally derived from PKR knockout mice produced in the Weissmann laboratory (35). Baltzis et al. (36) showed that MEF cells isolated from those mice can express an N-terminal-deleted isoform of PKR. We therefore designate these cells herein as PKR N^- MEFs. The PKR N^- MEFs were grown in DMEM containing 10% heat-inactivated fetal bovine serum (FBS). Wild type HT1080 and HT1080 PKR knockout cells (HT 1080 huPKR KO) were kindly provided by Malathi Krishnamurthy, University of Toledo, Ohio (55) and were grown in DMEM/10% FBS. Mouse PKR knockout MEFs stably transfected with empty vector ($PKR^{-/-}$ vector) or full-length human PKR ($PKR^{-/-}$ huPKR) were kindly provided by Dr. Gokhan Hotamisligil, Harvard University (38) and were maintained in DMEM/10% FBS. These cells were derived from PKR knockout mice produced in the Bell laboratory (56). Baltzis et al. (36) showed that MEF cells isolated from those mice can express a C-terminal-deleted isoform of PKR. We therefore designate these cells herein as PKR C^- MEFs.

We generated a new strain of mice knocked out for PKR as follows. The University of Michigan Transgenic Animal Core performed *in vitro* fertilization (IVF) with eggs from a C57BL/6J female mouse and sperm from a male mouse heterozygous for a CRISPR/Cas9 edited eIF2ak2 (PKR) gene. The sperm for the IVF was from this strain: C57BL/6NCrl-Eif2ak2$^{em1(IMPC)Mbp}$/Mmucd (RRID: MMRRC_050636-UCD); the sperm was obtained from the Mutant Mouse Resource and Research Center (MMRRC) at University of California at Davis, an NIH-funded strain repository. The strain was donated to the MMRRC by Kent Lloyd, D.V.M., University of California, Davis. We intercrossed progeny carrying the mutation through the N3 generation, and homozygotes were identified by PCR with the MMRRC genotyping assay and then mated. The full strain name of our mice is B6/J;C57BL/6NCrl-Eif2ak2$^{em1(IMPC)Mbp}$/Mmucd. We designate the strain PKR-TKO herein, and its characterization will be described elsewhere (D. Edwards and K. Spindler, unpublished data). A pregnant female from a homozygous mating of PKR-TKO mice was euthanized at day 15 to make mouse embryo fibroblasts. Embryos were dissected to remove viscera and trypsinized. We plated cells at a density of 1 embryo per 150 mm plate and passed them using a standard 3T3 protocol: cell density of 3.5×10^5cells per 60 mm plate, passaged every 3 days (53). After immortalization, cells were maintained in DMEM/10% FBS. The cells are designated PKR-TKO MEFs and were shown by immunoblot to not express mouse PKR, as expected (Figs. 2 and 4).

Wild-type MAV-1 virus stock was prepared and titrated on mouse NIH 3T6 fibroblasts as described previously (57). HAdV2 stock was prepared and titrated by plaque assay on HeLa cells. For all infections, the medium was removed, and the monolayer was washed with PBS. The virus inoculum was added for

1 h of adsorption at 37°C at MOI 5 in a small volume, and then medium containing 2% of the relevant serum was added without removing the inoculum.

Protein extraction. Total lysates were obtained by washing in phosphate-buffered saline (PBS), scraping, and pelleting the cells from a 6-well plate. Cell pellets from individual wells were incubated with 100 μl Pierce RIPA lysis buffer (Thermo Scientific, 89900) containing 1X protease inhibitors (Thermo Scientific, 78410) for 1 h on ice. Cell debris was removed by centrifugation at 14,000 $\times$ *g*, 10 min, 4°C. Total lysates were boiled 5 min in 1X Laemmli sample buffer (Bio-Rad, 1610737) containing 10% 2-mercaptoethanol (Sigma, M6250) and stored at −20°C.

Proteasome and cullin neddylation inhibition. For proteasome inhibition, NIH 3T6 fibroblasts were infected with MAV-1 at MOI 5 for 24 h and treated with 1, 5 or 10 μM MG132 (Sigma, M7449) in DMSO or DMSO alone (Sigma, D2650) for 6 h prior to harvesting. For cullin neddylation studies, NIH 3T6 fibroblasts were infected with MAV-1 at MOI 5 for 24 h and treated with 1, 3 or 5 μM MLN4924 (Cayman Chemical, 15217) in DMSO or DMSO alone for 24 h. Cell pellets were obtained by washing in 1X PBS, scraping and pelleting cells. Total protein lysates were obtained as described above in the protein extraction section and processed for immunoblot analysis. ImageJ software was used to quantify E1A protein relative to β actin.

Transfection. Subconfluent cells (HT1080 huPKR KO, cells; PKR N$^-$ or PKR TKOMEFs) were washed and incubated with a mix of DNA and Lipofectamine 2000 (1:4 DNA/Lipofectamine 2000) (Invitrogen, 11668-019) for 6 h, 37°C per the manufacturer's recommendations. Total DNA was always adjusted to 8 μg per 60 mm-plate with empty vector as necessary. The DNA-Lipofectamine 2000 mix was removed and DMEM/10% FBS was added. Cells were harvested by scraping and pelleting at 24 h posttransfection, followed by lysis as described above and processed for immunoblot as described below.

The pFlag-PKR plasmid was generated by GenScript (NJ, USA) using the following primers to amplify mouse PKR: forward 5′-AAG GCT AGC GGG GGC CCT CTAG-3′ and reverse 5′-CTT GGT ACC GCG GCC TAC-3′, this produced a fragment of mouse PKR cDNA with the 5′ UTR directly preceding it and a Flag tag at the C-terminus. The PCR product was inserted into pcDNA3.1(-) using NheI and KpnI restriction enzymes, whose recognition sites are underlined in the primer sequences, respectively.

The pFlag-E1B 55k plasmid was obtained by amplifying MAV-1 E1B, and a Flag tag was added to the C-terminal end by PCR using the following primers: forward 5′-AAG AAG CTT ATG GAG GAC CGT CAA GCT CTC-3′, reverse 5′-ATT GCG GCC TAC TTG TCG TCA TCG TCT TTG TAG TCT TCA CTC AAT TCC TCC-3′. The fragment was inserted into pcDNAI/Amp using HindIII and NotI restriction enzymes, whose recognition sites are underlined in the primer sequences, respectively.

Plasmids Flag-E4orf6, Flag-E4orf6 Y69R, Flag-E4orf6 V73K, Flag-E4orf6 L77K and Flag-E4orf6 Y69R/V73K/L77K (24) were kindly provided by Paola Blanchette, McGill University, Canada. We found an additional mutation in the plasmid Flag-E4orf6 Y69R/V73K/L77K in the position 103 (L103A) and we corrected this mutation to the wild type sequence using site-directed mutagenesis kit (E0554S, New England Biolabs) with the following primers: FW: 5′-AGTTTGGAGCCTGCATTGCCAC-3′, RV: 5′-TCATCCCCGGTCACGTAG-3′. We used DNA sequencing to confirm the presence of sequence encoding only the three amino acid changes Y69R, V73K, and L77K and that the position 103 corresponds to the wild type sequence (Eton Bioscience). This new plasmid with only 3 amino acid changes is designated FLAGmE4orf6TMWT8. Note that the true amino acid numbering is used here to designate the amino acids altered in the mutants (see the text).

Immunoblots. Total lysates from infected or transfected cells (3T6, PKR C$^-$ MEFs, PKR N$^-$ MEFs, HT1080 wt, HT1080 PKR KO, and PKR TKO MEFs) were prepared as described above. Lysates were analyzed by sodium dodecyl sulfate-polyacrylamide gel electrophoresis (SDS-PAGE) and immunoblotting. Equal volumes of total lysates were loaded on 10% acrylamide gels (8.3 cm wide x 7.3 cm high x 0.1 cm thick) and electrophoresed for 30 min at 10 mA for the 6% stacking gel and 90 min at 20 mA for the running gel. Gels were transferred to a polyvinylidene difluoride (PVDF) membrane (Bio-Rad, 1620177) for 1.5 h at 400 mA. Blots were blocked with 10% nonfat milk in Tris-buffered saline (50 mM Tris-HCl, pH 7.6; 150 mM NaCl) – 0.1% Tween 20 (Sigma, P1379) for 1 h at room temperature and probed with primary antibodies. Bands were visualized by Kwik Quant Western blot kit (Kindle Biosciences, R1004) and photos were taken with a Kwik Quant Imager. Photos were visualized and cropped using Adobe Photoshop CC 2021.

Antibodies. Primary antibodies used to detect MAV-1 E1A were mouse monoclonal 10b10 (58). Mouse monoclonal anti-PKR, B-10 (Santa Cruz Biotechnology, sc-6282) recognizes human and mouse PKR (https://datasheets.scbt.com/sc-6282.pdf). We also used a mouse monoclonal anti-β-actin (Santa Cruz Biotechnology, sc-1616) and anti-cullin 2 (Santa Cruz Biotechnology, sc-166506). The anti-HAdV 2 DBP antibody was a kind gift of Daniel Klessig (Cornell University) and was used at 1:250 dilution. GenScript (NJ, USA) generated the custom rabbit polyclonal antisera anti-MAV-1 E4orf6 (7871) and anti-MAV-1 E1B 55k (80623). For 7871, rabbits were immunized with MAV-1 E4orf6 peptides (106-CHCGRQGSLQVGPRR-120 and 247-SGSSPLIPGFDIPRC-260 coupled to keyhole limpet hemocyanin (KLH). For 80623, the immunogens were E1B 55k peptides (172-HWADDEGVNFERLA-185 and 417-PDRTRFTVDVEELS-430). Antibodies were purified by affinity chromatography using the respective peptides for each immunogen. The 7871 and 80623 antisera specificities were validated by immunoprecipitation from *in vitro* transcription-translation reactions using plasmids encoding MAV-1 E4orf6, MAV-1 E1B 55k, or control empty vectors as templates (data not shown).

Immunoprecipitation. PKR N$^-$ MEFs, HT1080 huPKR KO cells or PKR TKO MEFs were transfected with pFlag-E1B 55k, pFlag-E4orf6 and pFlag-PKR plasmids, samples were lysed as described above, and supernatants were obtained by centrifugation. Supernatants were precleared by incubation for 1 h at 4°C with protein A-coupled beads that had been equilibrated in RIPA buffer containing protease inhibitors (EMD Millipore, 16-125). After pelleting and removal of the beads, samples were then incubated with

anti-E1B 55k (80623, 1:100) overnight at 4°C. Protein A-coupled beads were added to the samples and incubated for 2 h, 4°C. Beads were washed three times with E1A buffer (250 mM NaCl; 50 mM Tris HCl pH 7.4; 0.1% NP40) and one time with 50 mM Tris HCl pH 7.4. Finally, beads were boiled for 5 min in Laemmli sample buffer/10% 2-mercaptoethanol. Samples were stored at −20°C for immunoblot processing.

ACKNOWLEDGMENTS

We thank Paola Blanchette (McGill University, Canada) for E4orf6 plasmids, Malathi Krishnamurthy (University of Toledo, Ohio) for human HT1080 PKR knockout cells, Daniel Klessig (Cornell University, New York) for the HAdV-2 DBP mouse monoclonal antibody, Robert Silverman (Cleveland Clinic, Ohio) for PKR N^- MEF cells and Gokhan Hotamisligil (Harvard School of Public Health, Massachusetts) for PKR C^- MEF cells expressing empty vector or huPKR. We thank Thom Saunders and the University of Michigan Transgenic Model Core for advice and generation of the PKR-TKO mice. We thank Daniel Edwards, Shivani Gupta, Carla Pretto-Kernahan, and Irene Althaus for technical assistance. We thank Michael Imperiale and Jason Weinberg for helpful comments on the manuscript.

This work was supported by HHS/NIH/National Institute of Allergy and Infectious Diseases (NIAID) R01AI133935 and a University of Michigan Endowment for the Basic Sciences Accelerator Award U069440 to Katherine R. Spindler.

REFERENCES

1. Ball AO, Williams ME, Spindler KR. 1988. Identification of mouse adenovirus type 1 early region 1: DNA sequence and a conserved transactivating function. J Virol 62:3947–3957. https://doi.org/10.1128/JVI.62.11.3947-3957.1988.
2. Temple M, Antoine G, Delius H, Stahl S, Winnacker E-L. 1981. Replication of mouse adenovirus strain FL DNA. Virology 109:1–12. https://doi.org/10.1016/0042-6822(81)90466-9.
3. Kajon AE, Brown CC, Spindler KR. 1998. Distribution of mouse adenovirus type 1 in intraperitoneally and intranasally infected adult outbred mice. J Virol 72:1219–1223. https://doi.org/10.1128/JVI.72.2.1219-1223.1998.
4. Guida JD, Fejer G, Pirofski L-A, Brosnan CF, Horwitz MS. 1995. Mouse adenovirus type 1 causes a fatal hemorrhagic encephalomyelitis in adult C57BL/6 but not BALB/c mice. J Virol 69:7674–7681. https://doi.org/10.1128/JVI.69.12.7674-7681.1995.
5. Ashley SL, Welton AR, Harwood KM, Van Rooijen N, Spindler KR. 2009. Mouse adenovirus type 1 infection of macrophages. Virology 390:307–314. https://doi.org/10.1016/j.virol.2009.05.025.
6. Charles PC, Guida JD, Brosnan CF, Horwitz MS. 1998. Mouse adenovirus type-1 replication is restricted to vascular endothelium in the CNS of susceptible strains of mice. Virology 245:216–228. https://doi.org/10.1006/viro.1998.9180.
7. Hsu T-H, Spindler KR. 2012. Identifying host factors that regulate viral infection. PLoS Pathog 8:e1002772. https://doi.org/10.1371/journal.ppat.1002772.
8. Gralinski LE, Ashley SL, Dixon SD, Spindler KR. 2009. Mouse adenovirus type 1-induced breakdown of the blood-brain barrier. J Virol 83:9398–9410. https://doi.org/10.1128/JVI.00954-09.
9. Smith K, Brown CC, Spindler KR. 1998. The role of mouse adenovirus type 1 early region 1A in acute and persistent infections in mice. J Virol 72:5699–5706. https://doi.org/10.1128/JVI.72.7.5699-5706.1998.
10. Weinberg JB, Jensen DR, Gralinski LE, Lake AR, Stempfle GS, Spindler KR. 2007. Contributions of E1A to mouse adenovirus type 1 pathogenesis following intranasal inoculation. Virology 357:54–67. https://doi.org/10.1016/j.virol.2006.08.013.
11. Spindler KR, Moore ML, Cauthen AN. 2007. Mouse adenoviruses, p 49–65. *In* Fox JG, Barthold SW, Davisson MT, Newcomer CE, Quimby FW, Smith AL (ed), The mouse in biomedical research, 2nd ed, vol 2. Academic Press, New York.
12. Hemmi S, Spindler KR. 2019. Murine adenoviruses: Tools for studying adenovirus pathogenesis in a natural host. FEBS Lett 593:3649–3659. https://doi.org/10.1002/1873-3468.13699.
13. Kitajewski J, Schneider RJ, Safer B, Munemitsu SM, Samuel CE, Thimmappaya B, Shenk T. 1986. Adenovirus VAI RNA antagonizes the antiviral action of interferon by preventing activation of the interferon-induced eIF-2 alpha kinase. Cell 45:195–200. https://doi.org/10.1016/0092-8674(86)90383-1.
14. Maran A, Mathews MB. 1988. Characterization of the double-stranded RNA implicated in the inhibition of protein synthesis in cells infected with a mutant adenovirus defective for VA RNA. Virology 164:106–113. https://doi.org/10.1016/0042-6822(88)90625-3.
15. Meissner JD, Hirsch GN, LaRue EA, Fulcher RA, Spindler KR. 1997. Completion of the DNA sequence of mouse adenovirus type 1: Sequence of E2B, L1, and L2 (18–51 map units). Virus Res 51:53–64. https://doi.org/10.1016/s0168-1702(97)00079-8.
16. Goodman DE, Pretto CD, Krepostman TA, Carnahan KE, Spindler KR. 2019. Enhanced replication of mouse adenovirus type 1 following virus-induced degradation of protein kinase R (PKR). mBio 10:e00668-19. https://doi.org/10.1128/mBio.00668-19.
17. Querido E, Morrison MR, Chu-Pham-Dang H, Thirlwell SW, Boivin D, Branton PE, Morisson MR. 2001. Identification of three functions of the adenovirus E4orf6 protein that mediate p53 degradation by the E4orf6-E1B55K complex. J Virol 75:699–709. https://doi.org/10.1128/JVI.75.2.699-709.2001.
18. Stracker TH, Carson CT, Weitzman MD. 2002. Adenovirus oncoproteins inactivate the Mre11-Rad50-NBS1 DNA repair complex. Nature 418:348–352. https://doi.org/10.1038/nature00863.
19. Orazio NI, Naeger CM, Karlseder J, Weitzman MD. 2011. The adenovirus E1b55K/E4orf6 complex induces degradation of the Bloom helicase during infection. J Virol 85:1887–1892. https://doi.org/10.1128/JVI.02134-10.
20. Gupta A, Jha S, Engel DA, Ornelles DA, Dutta A. 2013. Tip60 degradation by adenovirus relieves transcriptional repression of viral transcriptional activator EIA. Oncogene 32:5017–5025. https://doi.org/10.1038/onc.2012.534.
21. Herrmann C, Dybas JM, Liddle JC, Price AM, Hayer KE, Lauman R, Purman CE, Charman M, Kim ET, Garcia BA, Weitzman MD. 2020. Adenovirus-mediated ubiquitination alters protein-RNA binding and aids viral RNA processing. Nat Microbiol 5:1217–1231. https://doi.org/10.1038/s41564-020-0750-9.
22. Dallaire F, Blanchette P, Groitl P, Dobner T, Branton PE. 2009. Identification of integrin alpha3 as a new substrate of the adenovirus E4orf6/E1B 55-kilodalton E3 ubiquitin ligase complex. J Virol 83:5329–5338. https://doi.org/10.1128/JVI.00089-09.
23. Schreiner S, Kinkley S, Burck C, Mund A, Wimmer P, Schubert T, Groitl P, Will H, Dobner T. 2013. SPOC1-mediated antiviral host cell response is antagonized early in human adenovirus type 5 infection. PLoS Pathog 9:e1003775. https://doi.org/10.1371/journal.ppat.1003775.
24. Gilson T, Blanchette P, Ballmann MZ, Papp T, Pénzes JJ, Benkő M, Harrach B, Branton PE. 2016. Using the E4orf6-based E3 ubiquitin ligase as a tool to analyze the evolution of adenoviruses. J Virol 90:7350–7367. https://doi.org/10.1128/JVI.00420-16.

25. Galabru J, Hovanessian A. 1987. Autophosphorylation of the protein kinase dependent on double-stranded RNA. J Biol Chem 262:15538–15544. https://doi.org/10.1016/S0021-9258(18)47759-9.
26. Garcia MA, Gil J, Ventoso I, Guerra S, Domingo E, Rivas C, Esteban M. 2006. Impact of protein kinase PKR in cell biology: From antiviral to antiproliferative action. Microbiol Mol Biol Rev 70:1032–1060. https://doi.org/10.1128/MMBR.00027-06.
27. Verma IM, Stevenson JK, Schwarz EM, Van Antwerp D, Miyamoto S. 1995. Rel/NF-kappa B/I kappa B family: intimate tales of association and dissociation. Genes Dev 9:2723–2735. https://doi.org/10.1101/gad.9.22.2723.
28. Duda DM, Borg LA, Scott DC, Hunt HW, Hammel M, Schulman BA. 2008. Structural insights into NEDD8 activation of cullin-RING ligases: conformational control of conjugation. Cell 134:995–1006. https://doi.org/10.1016/j.cell.2008.07.022.
29. Saha A, Deshaies RJ. 2008. Multimodal activation of the ubiquitin ligase SCF by Nedd8 conjugation. Mol Cell 32:21–31. https://doi.org/10.1016/j.molcel.2008.08.021.
30. Boh BK, Smith PG, Hagen T. 2011. Neddylation-induced conformational control regulates cullin RING ligase activity in vivo. J Mol Biol 409:136–145. https://doi.org/10.1016/j.jmb.2011.03.023.
31. Brownell JE, Sintchak MD, Gavin JM, Liao H, Bruzzese FJ, Bump NJ, Soucy TA, Milhollen MA, Yang X, Burkhardt AL, Ma J, Loke HK, Lingaraj T, Wu D, Hamman KB, Spelman JJ, Cullis CA, Langston SP, Vyskocil S, Sells TB, Mallender WD, Visiers I, Li P, Claiborne CF, Rolfe M, Bolen JB, Dick LR. 2010. Substrate-assisted inhibition of ubiquitin-like protein-activating enzymes: the NEDD8 E1 inhibitor MLN4924 forms a NEDD8-AMP mimetic in situ. Mol Cell 37:102–111. https://doi.org/10.1016/j.molcel.2009.12.024.
32. Soucy TA, Smith PG, Milhollen MA, Berger AJ, Gavin JM, Adhikari S, Brownell JE, Burke KE, Cardin DP, Critchley S, Cullis CA, Doucette A, Garnsey JJ, Gaulin JL, Gershman RE, Lublinsky AR, McDonald A, Mizutani H, Narayanan U, Olhava EJ, Peluso S, Rezaei M, Sintchak MD, Talreja T, Thomas MP, Traore T, Vyskocil S, Weatherhead GS, Yu J, Zhang J, Dick LR, Claiborne CF, Rolfe M, Bolen JB, Langston SP. 2009. An inhibitor of NEDD8-activating enzyme as a new approach to treat cancer. Nature 458:732–736. https://doi.org/10.1038/nature07884.
33. Querido E, Marcellus RC, Lai A, Charbonneau R, Teodoro JG, Ketner G, Branton PE. 1997. Regulation of p53 levels by the E1B 55-kilodalton protein and E4orf6 in adenovirus-infected cells. J Virol 71:3788–3798. https://doi.org/10.1128/JVI.71.5.3788-3798.1997.
34. Baker A, Rohleder KJ, Hanakahi LA, Ketner G. 2007. Adenovirus E4 34k and E1b 55k oncoproteins target host DNA ligase IV for proteasomal degradation. J Virol 81:7034–7040. https://doi.org/10.1128/JVI.00029-07.
35. Yang YL, Reis LF, Pavlovic J, Aguzzi A, Schafer R, Kumar A, Williams BR, Aguet M, Weissmann C. 1995. Deficient signaling in mice devoid of double-stranded RNA-dependent protein kinase. EMBO J 14:6095–6106. https://doi.org/10.1002/j.1460-2075.1995.tb00300.x.
36. Baltzis D, Li S, Koromilas AE. 2002. Functional characterization of *pkr* gene products expressed in cells from mice with a targeted deletion of the N terminus or C terminus domain of PKR. J Biol Chem 277:38364–38372. https://doi.org/10.1074/jbc.M203564200.
37. Kring SC, Ball AO, Spindler KR. 1992. Transcription mapping of mouse adenovirus type 1 early region 4. Virology 190:248–255. https://doi.org/10.1016/0042-6822(92)91211-c.
38. Nakamura T, Kunz RC, Zhang C, Kimura T, Yuan CL, Baccaro B, Namiki Y, Gygi SP, Hotamisligil GS. 2015. A critical role for PKR complexes with TRBP in Immunometabolic regulation and eIF2alpha phosphorylation in obesity. Cell Rep 11:295–307. https://doi.org/10.1016/j.celrep.2015.03.021.
39. Cesaro T, Michiels T. 2021. Inhibition of PKR by viruses. Front Microbiol 12:757238. https://doi.org/10.3389/fmicb.2021.757238.
40. Weitzman MD, Ornelles DA. 2005. Inactivating intracellular antiviral responses during adenovirus infection. Oncogene 24:7686–7696. https://doi.org/10.1038/sj.onc.1209063.
41. Carson CT, Schwartz RA, Stracker TH, Lilley CE, Lee DV, Weitzman MD. 2003. The Mre11 complex is required for ATM activation and the G2/M checkpoint. EMBO J 22:6610–6620. https://doi.org/10.1093/emboj/cdg630.
42. Schreiner S, Wimmer P, Sirma H, Everett RD, Blanchette P, Groitl P, Dobner T. 2010. Proteasome-dependent degradation of Daxx by the viral E1B-55K protein in human adenovirus-infected cells. J Virol 84:7029–7038. https://doi.org/10.1128/JVI.00074-10.
43. Blackford AN, Patel RN, Forrester NA, Theil K, Groitl P, Stewart GS, Taylor AM, Morgan IM, Dobner T, Grand RJ, Turnell AS. 2010. Adenovirus 12 E4orf6 inhibits ATR activation by promoting TOPBP1 degradation. Proc Natl Acad Sci U S A 107:12251–12256. https://doi.org/10.1073/pnas.0914605107.
44. Ikegami T, Narayanan K, Won S, Kamitani W, Peters CJ, Makino S. 2009. Rift Valley fever virus NSs protein promotes post-transcriptional downregulation of protein kinase PKR and inhibits eIF2alpha phosphorylation. PLoS Pathog 5:e1000287. https://doi.org/10.1371/journal.ppat.1000287.
45. Kalveram B, Ikegami T. 2013. Toscana virus NSs protein promotes degradation of double-stranded RNA-dependent protein kinase. J Virol 87:3710–3718. https://doi.org/10.1128/JVI.02506-12.
46. Feng GS, Chong K, Kumar A, Williams BR. 1992. Identification of double-stranded RNA-binding domains in the interferon-induced double-stranded RNA-activated p68 kinase. Proc Natl Acad Sci U S A 89:5447–5451. https://doi.org/10.1073/pnas.89.12.5447.
47. Farrell PJ, Balkow K, Hunt T, Jackson RJ, Trachsel H. 1977. Phosphorylation of initiation factor eIF-2 and the control of reticulocyte protein synthesis. Cell 11:187–200. https://doi.org/10.1016/0092-8674(77)90330-0.
48. Jacobs BL, Langland JO. 1996. When two strands are better than one: the mediators and modulators of the cellular responses to double-stranded RNA. Virology 219:339–349. https://doi.org/10.1006/viro.1996.0259.
49. Price AM, Steinbock RT, Di C, Hayer KE, Li Y, Herrmann C, Parenti NA, Whelan JN, Weiss SR, Weitzman MD. 2021. Adenovirus prevents dsRNA formation by promoting efficient splicing of viral RNA. Nucleic Acids Res doi:10.1093/nar/gkab896.
50. Ponia SS, Robertson SJ, McNally KL, Subramanian G, Sturdevant GL, Lewis M, Jessop F, Kendall C, Gallegos D, Hay A, Schwartz C, Rosenke R, Saturday G, Bosio CM, Martens C, Best SM. 2021. Mitophagy antagonism by ZIKV reveals Ajuba as a regulator of PINK1 signaling, PKR-dependent inflammation, and viral invasion of tissues. Cell Rep 37:109888. https://doi.org/10.1016/j.celrep.2021.109888.
51. Patel RC, Sen GC. 1998. PACT, a protein activator of the interferon-induced protein kinase, PKR. EMBO J 17:4379–4390. https://doi.org/10.1093/emboj/17.15.4379.
52. Lee ES, Yoon CH, Kim YS, Bae YS. 2007. The double-strand RNA-dependent protein kinase PKR plays a significant role in a sustained ER stress-induced apoptosis. FEBS Lett 581:4325–4332. https://doi.org/10.1016/j.febslet.2007.08.001.
53. Todaro GJ, Green H. 1963. Quantitative studies of the growth of mouse embryo cells in culture and their development into established lines. J Cell Biol 17:299–313. https://doi.org/10.1083/jcb.17.2.299.
54. Sawicki DL, Silverman RH, Williams BR, Sawicki SG. 2003. Alphavirus minus-strand synthesis and persistence in mouse embryo fibroblasts derived from mice lacking RNase L and protein kinase R. J Virol 77:1801–1811. https://doi.org/10.1128/jvi.77.3.1801-1811.2003.
55. Manivannan P, Siddiqui MA, Malathi K. 2020. RNase L amplifies interferon signaling by inducing protein kinase R-mediated antiviral stress granules. J Virol 94:e00205-20. https://doi.org/10.1128/JVI.00205-20.
56. Abraham N, Stojdl DF, Duncan PI, Methot N, Ishii T, Dube M, Vanderhyden BC, Atkins HL, Gray DA, McBurney MW, Koromilas AE, Brown EG, Sonenberg N, Bell JC. 1999. Characterization of transgenic mice with targeted disruption of the catalytic domain of the double-stranded RNA-dependent protein kinase, PKR. J Biol Chem 274:5953–5962. https://doi.org/10.1074/jbc.274.9.5953.
57. Cauthen AN, Welton AR, Spindler KR. 2007. Construction of mouse adenovirus type 1 mutants. Methods Mol Med 130:41–59. https://doi.org/10.1385/1-59745-166-5:41.
58. Fang L, Stevens JL, Berk AJ, Spindler KR. 2004. Requirement of Sur2 for efficient replication of mouse adenovirus type 1. J Virol 78:12888–12900. https://doi.org/10.1128/JVI.78.23.12888-12900.2004.